

1 **Distinct types of short open reading frames are translated in** 2 **plant cells**

3 Igor Fesenko^{1,*}, Ilya Kirov¹, Andrey Kniazev¹, Regina Khazigaleeva¹, Vassili Lazarev², Daria
4 Kharlampieva², Ekaterina Grafaskaia², Viktor Zgoda³, Ivan Butenko², Georgy Arapidi¹, Anna Mamaeva¹,
5 Vadim Ivanov¹, Vadim Govorun^{1,2}.

6 ¹ *Laboratory of Proteomics, Shemyakin and Ovchinnikov Institute of Bioorganic Chemistry, Moscow,*
7 *Russian Federation;* ² *Federal Research and Clinical Centre of Physical-Chemical Medicine, Moscow,*
8 *Russian Federation;* ³ *Laboratory of System Biology, Institute of Biomedical Chemistry, Moscow, Russian*
9 *Federation.*

10

11 **Corresponding author(s).**

12 * Igor Fesenko, e-mail: fesigor@gmail.com

13

14 **Running title:** Genome-wide translation of sORFs in plants

15

16 **Keywords:** short open reading frames, plant peptides, LC-MS/MS, evolution, alternative splicing,
17 lncRNA

18

19

ABSTRACT

20 Genomes contain millions of short (<100 codons) open reading frames (sORFs), which are usually
21 dismissed during gene annotation. Nevertheless, peptides encoded by such sORFs can play important
22 biological roles, and their impact on cellular processes has long been underestimated. Here, we
23 analyzed approximately 70,000 transcribed sORFs in the model plant *Physcomitrella patens* (moss).
24 Several distinct classes of sORFs that differ in terms of their position on transcripts and the level of
25 evolutionary conservation are present in the moss genome. Over 5000 sORFs were conserved in at

26 least one of ten plant species examined. Mass spectrometry analysis of proteomic and peptidomic
27 datasets suggested that 584 sORFs located on distinct parts of mRNAs and long non-coding RNAs
28 (lncRNAs) are translated, including 73 conservative sORFs. Translational analysis of the sORFs and
29 main ORFs at a single locus suggested the existence of genes that code for multiple proteins and
30 peptides with tissue-specific expression. Alternative splicing is likely involved in the excision of
31 translatable sORFs from such transcripts. We identified a group of sORFs homologous to known
32 protein domains and suggested they function as small interfering peptides. Functional analysis of
33 candidate lncRNA-encoded peptides showed it to be involved in regulating growth and
34 differentiation in moss. The high evolutionary rate and wide translation of sORFs suggest that they
35 may provide a reservoir of potentially active peptides and their importance as a raw material for
36 gene evolution. Our results thus open new avenues for discovering novel, biologically active peptides
37 in the plant kingdom.

38

39

INTRODUCTION

40

41 The genomes of nearly all organisms contain hundreds of thousands of short open reading
42 frames (sORFs; <100 codons) whose coding potential has been the subject of recent reviews
43 (Andrews and Rothnagel 2014; Couso 2015; Hellens et al. 2016; Couso and Patraquim 2017).
44 However, gene annotation algorithms are generally not suited for dealing with sORFs because short
45 sequences are unable to obtain high conservation scores, which serve as an indicator of functionality
46 (Ladoukakis et al. 2011). Nevertheless, using various bioinformatic approaches, sORFs with high
47 coding potential have been identified in a range of organisms including fruit flies, mice, yeast and
48 *Arabidopsis thaliana* (Ladoukakis et al. 2011; Hanada et al. 2013; Aspden et al. 2014; Bazzini et al.
49 2014). The first systematic study of sORFs was conducted on baker's yeast, where 299 previously
50 non-annotated sORFs were identified and tested in genetic experiments (Kastenmayer et al. 2006).
51 Subsequently, 4561 conserved sORFs were identified in the genus *Drosophila*, 401 of which were
52 postulated to be functional, taking into account their syntenic positions, low K_A/K_S (<0.1) values and

53 transcriptional evidence (Ladoukakis et al. 2011). In a recent study, Mackowiak and colleagues
54 predicted the presence of 2002 novel conserved sORFs (from 9 to 101 codons) in *H. sapiens*, *M.*
55 *musculus*, *D. rerio*, *D. melanogaster* and *C. elegans* (Mackowiak et al. 2015). The first comprehensive
56 study of sORFs in plants postulated the existence of thousands of sORFs with high coding potential in
57 *Arabidopsis* (Lease and Walker 2006; Hanada et al. 2007; Hanada et al. 2013), including 49 that
58 induced various morphological changes and had visible phenotypic effects.

59 Recent studies have pointed to the important roles of sORF-encoded peptides (SEPs) in
60 cells (Magny et al. 2013; Nelson et al. 2016; D'Lima et al. 2017; Huang et al. 2017; Matsumoto et al.
61 2017). However, unraveling the roles of SEPs is a challenging task, as is their detection at the
62 biochemical level. In animals, SEPs are known play important roles in a diverse range of cellular
63 processes (Kondo et al. 2010; Magny et al. 2013). By contrast, only a few functional SEPs have been
64 reported in plants, including POLARIS (PLS; 36 amino acids), EARLY NODULIN GENE 40 (ENOD40;
65 12, 13, 24 or 27 amino acids), ROTUNDIFOLIA FOUR (ROT4; 53 amino acids), KISS OF DEATH (KOD;
66 25 amino acids), BRICK1 (BRK1; 84 amino acids), Zm-908p11 (97 amino acids) and Zm-401p10 (89
67 amino acids) (Andrews and Rothnagel 2014; Tavormina et al. 2015). These SEPs help modulate root
68 growth and leaf vascular patterning (Chilley et al. 2006), symbiotic nodule development (Djordjevic
69 et al. 2015), polar cell proliferation in lateral organs and leaf morphogenesis (Narita et al. 2004), and
70 programmed cell death (apoptosis) (Blanvillain et al. 2011).

71 To date, functional sORFs have been found in a variety of transcripts, including
72 untranslated regions of mRNA (5' leader and 3' trailer sequences), lncRNAs, and microRNA
73 transcripts (pri-miRNAs) (Andrews and Rothnagel 2014; Laing et al. 2015; Lauressergues et al. 2015;
74 Couso and Patraquim 2017). Evidence for the transcription of potentially functional sORFs has been
75 obtained in *Populus deltoides*, *Phaseolus vulgaris*, *Medicago truncatula*, *Glycine max* and *Lotus*
76 *japonicus* (Guillen et al. 2013). The transcription of sORFs can be regulated by stress conditions and
77 depends on the developmental stage of the plant (De Coninck et al. 2013; Hanada et al. 2013;
78 Rasheed et al. 2016). Indeed, sORFs might represent an important source of advanced traits required
79 under stress conditions. During stress, genomes undergo widespread transcription to produce a
80 diverse range of RNAs (Kim et al. 2010; Mazin et al. 2014); therefore, a large portion of sORFs

81 becomes accessible to the translation machine for peptide production. Stress conditions can lead to
82 the transcription of sORFs located in genomic regions that are usually non-coding (Giannakakis et al.
83 2015). Such sORFs appear to serve as raw materials for the birth and subsequent evolution of new
84 protein-coding genes (Couso and Patraquim 2017).

85 The transcription of an sORF does not necessarily indicate that it fulfills any biological
86 role, as opposed to being a component of the so-called translational noise (Guttman et al. 2013).
87 According to ribosomal profiling data, thousands of lncRNAs display high ribosomal occupancy in
88 regions containing sORFs in mammals (Ingolia et al. 2011; Aspden et al. 2014; Bazzini et al. 2014).
89 However, lncRNAs can have the same ribosome profiling patterns as canonical non-coding RNAs
90 (e.g., rRNA) that are known not to be translated, implying that these lncRNAs are unlikely to produce
91 functional peptides (Guttman et al. 2013). In addition, identification of SEPs via mass spectrometry
92 analyses has found many fewer peptides than predicted sORFs (Slavoff et al. 2013; Aspden et al.
93 2014). Thus, the abundance, lifetime and other features of SEPs are generally unclear.

94 We performed a comprehensive analysis of the sORFs that have canonical AUG start
95 codons and high coding potential in the *Physcomitrella patens* genome. The translation of hundreds
96 of sORFs was confirmed by mass-spectrometry analysis. From these, candidate lncRNA-encoded
97 peptides were selected for further analysis, which provided evidence for their biological functions.

98 RESULTS

99 **Discovery and classification of potential coding sORFs in the moss genome**

100 Our approach is summarized in Fig. 1A. At the first stage of analysis, we used the sORFinder tool
101 (Hanada et al. 2010) to identify single-exon sORFs starting with an AUG start codon and less than
102 300 bp long. This approach resulted in the identification of 638,439 sORFs with high coding potential
103 (CI index) in all regions of the *P. patens* genome.

104 We selected 70,095 unique sORFs located on transcripts annotated in the moss genome
105 (phytozome.jgi.doe.gov) and/or our dataset (Fesenko et al. 2015) for further analysis, as well as
106 those on lncRNAs from two databases -CantataDB (Szczesniak et al. 2016) and GreenC (Paytuvi
107 Gallart et al. 2016); sORFs located in repetitive regions were discarded (Supplemental Table S1).

108 These selected sORFs, which were 33 to 303 bp long, were located on 33,981 transcripts (22,969
109 genes), with up to 28 sORFs per transcript (Supplemental Fig. S1A).

110 We then classified the sORFs based on their location on the transcript: 63,109 “genic-sORFs”
111 (located on annotated transcripts, but not on lncRNA), 1241 “intergenic-sORFs” (located on
112 transcripts from our dataset and not annotated in the current version of the genome) and 5745
113 “lncRNA-sORFs” (located on lncRNAs from CantataDB (Szczesniak et al. 2016), GreenC (Paytuví
114 Gallart et al. 2016) or our data set (Fesenko et al. 2017); Fig. 1B). The genic-sORFs include 11,998
115 upstream ORFs (uORFs; for 5'-UTR location), 9443 downstream ORFs (dORFs; for 3'-UTR location),
116 36,731 coding sequence-sORFs (CDS-sORFs; sORFs overlapping with main ORFs (+1 frame) in non-
117 canonical +2 and +3 reading frames) and 3485 interlaced-sORFs (overlapping with both the CDS and
118 5'-UTR or CDS and 3'-UTR on the same transcript) (Fig. 1B, Supplemental Fig. S1B).

119 As expected based on the sORFinder search strategy (Hanada et al. 2010), the sORF set was
120 enriched in CDS-sORFs (52%, Fisher's exact test, P-value = 1.736392e-285), whereas dORFs, uORFs
121 and interlaced-sORFs were underrepresented (Fisher's exact test, P-value < 4.792689e-88)
122 compared to a random exonic fragments (REF) set, which was used as a negative control.

123 On average, CDS-sORFs (median size of 22 codons) were shorter than uORFs (median size of
124 35 codons; Mann-Whitney *U* test P = 2.2e-151) and dORFs (median length 32 codons, Mann-Whitney
125 *U* test P = 1.03e-43). The median size of interlaced-sORFs was 49 codons, which is significantly
126 longer than other genic-sORFs (Mann-Whitney *U* test P = 0.0021) (Fig. 1C).

127 Genes possessing CDS-sORFs were enriched in GO terms associated with protein binding and
128 transferase activity, while genes possessing uORFs were enriched for signal transduction and
129 transcriptional regulation (Supplemental Fig. S2). Such contrasting functional associations could be
130 reflective of evolutionary trends that result in distinct sORF groups within protein coding genes.

131

132 **Analysis of evolutionary conservation of sORFs**

133 It is widely accepted that evolutionary conservation is a strong indicator of functionality (Ladoukakis
134 et al. 2011). To estimate the number of conserved sORFs in the moss genome and the evolutionary
135 pressure on their amino acid sequences, we performed a tBLASTn search (e-value cutoff 0.00001) of

136 each sORF sequence against the reconstructed genomes of three *P. patens* ecotypes: Villersexel,
137 Reute, and Kaskasia as well as the transcriptomes of ten other species (Supplemental Fig. S3). The
138 selected species include those that diverged from *P. patens* 177 (*Ceratodon purpureus*), 320
139 (*Sphagnum fallax*), 493 (*Marchantia polymorpha*), 532 (*Arabidopsis thaliana*, *Oryza sativa*, *Zea mays*,
140 *Selaginella moellendorffii* and *Spirodela polyrhiza*) and 1160 (*Volvox carteri* and *Chlamydomonas*
141 *reinhardtii*) Mya (According to www.timetree.org (Kumar et al. 2017); Supplemental Fig. S3).

142 A conservation analysis of the sORFs in the reconstructed genomes of these ecotypes showed that
143 2.4% (1618) of the sORFs were lacking either the start or stop codons in at least one species.
144 Interestingly, CDS-sORFs (506) were significantly underrepresented in this set (Fisher's exact test P-
145 value < 2.2e-16), while uORF (478), dORF (278), lncRNA-sORFs (202), and intergenic-sORFs (59)
146 were significantly overrepresented (Fisher's exact test P-value < 2.2e-16). These results suggest that
147 uORFs, dORF, lncRNA-sORFs, and intergenic-sORFs are prone to a shorter retention time than CDS-
148 ORFs.

149 We found 5034 conserved sORFs with detectable homologous sequences in at least one
150 species: 4797 in *C. purpureus*, 1049 in *S. fallax*, 436 in *M. polymorpha*, 328 in *S. moellendorffii*, 297 in
151 *S. polyrhiza*, 275 in *A. thaliana*, 282 in *Z. mays*, 274 in *O. sativa*, 86 in *V. carteri* and 89 in *C. reinhardtii*.
152 The number of conserved sORFs was negatively correlated with the time since divergence, with the
153 fewest homologous sequences found in *V. carteri* and *C. reinhardtii*, which diverged more than 1000
154 Mya from a common ancestor. We found that lncRNA-sORFs were underrepresented among sORFs
155 having homologs in the ten species examined (Fig. 2A). We also found significantly fewer uORFs and
156 dORFs in the two closest species, *C. purpureus* and *S. fallax*, whereas CDS-sORFs were significantly
157 overrepresented in these species (Fisher's exact test, $P < 2.2e-16$) (Fig. 2B).

158 However, the portion of uORFs and dORFs found in the more distant species was increased relative
159 to the initial dataset compared to CDS-sORFs, causing their significant overrepresentation (Fisher's
160 exact test, $P < 0.0005$). Thus, the relative enrichment of conserved CDS-sORFs and interlaced-sORFs
161 found in the two closest species of *P. patens*, *C. purpureus* and *S. fallax*, resulted from a significant
162 reduction in the number of uORFs and dORFs (Fig. 2A). As a control, we also investigated changes in
163 the proportion of uREFs, dREFs and CDS-REFs in these ten species and obtained opposite results

164 (Supplemental Fig. S4). To compare this trend with that of the protein coding genes, we selected 158
165 annotated *P. patens* genes that code for small proteins without introns (< 100 aa). The percentages of
166 sORFs and these proteins showing homology with at least one species were significantly different
167 (7.2% sORFs vs. 86% small proteins), pointing to high genome turnover of sORF sequences.

168 We next assessed whether the lengths of homologous sORFs from other species were the same as
169 those in moss or if they varied in size. According to our data, most putative homologous sORFs
170 differed in length, contributing to sORF diversification (Supplemental Fig. S5).

171 To better understand the large-scale trends of sORF evolution, we examined the differences
172 in selection pressure at the amino acid level between different major groups of sORFs (CDS-sORFs,
173 uORFs, dORFs, lncRNA-sORFs, interlaced-sORFs) using the criterion of K_A/K_S . This analysis showed
174 that the highest portion of sORFs comprised CDS-sORFs, with K_A/K_S ratio > 1, implying ongoing
175 positive selection of sORFs emerging in the CDS of protein-coding genes. This criterion for other
176 sORF groups was < 1 in most cases, pointing to purifying selection for these sequences (Fig. 2C).

177 Thus, evolutionary analysis demonstrated that the conservation of an sORF on a large
178 evolutionary scale differs from that of randomly selected exon sequences and depends on the
179 location of the sORF. Higher retention rates were observed for uORFs and dORFs, whereas CDS-
180 sORFs and lncRNA-ORFs were under strong positive selection.

181

182 **Experimental evidence for the translation of sORFs**

183 Obtaining evidence for the translation of sORFs is an important step towards identifying functional
184 SEPs. We analyzed the Kozak consensus sequences (Kozak 1986) surrounding sORF start codons.
185 Kozak consensus sequence plays an important role in translation initiation (Kozak 1997). Depending
186 on the presence of the purine in position -3 and the G in position +4 (where +1 is “A” in the “AUG”
187 codon) the Kozak was considered to be “strong” (both are present), “medium” (one is present) or
188 “weak” (neither are present) (Kozak 1997). According to our results, 41816 (~60%) of the predicted
189 sORFs were surrounded by “strong” and “medium” Kozak sequences. These values were significantly
190 smaller than those of annotated protein coding ORFs (87%, Fisher’s exact test P-value < 2.2e-16).

191 We then verified the translation of our predicted sORFs using mass-spectrometry (MS) analysis.
192 Taking into account the shortage of proteomic methods for identifying small proteins or peptides, in
193 the current study, we generated two datasets: the “peptidomic” dataset - endogenous peptides
194 extracted from three types of moss cells: gametophores, protonemata and protoplasts and the
195 “proteomic” dataset - tryptic peptides generated in a standard proteomic pipeline (Supplemental
196 Table S2). All datasets were mapped with MaxQuant against a custom database containing our sORFs
197 together with nuclear, chloroplast and mitochondrial moss protein sequences (see details in the
198 Methods). PSMs (peptide spectrum matches) were identified at 1 % FDR, and ambiguous peptides
199 were filtered out. In total, we confirmed the translation of 584 sORFs: 198 in gametophores, 277 in
200 protonemata, and 190 in protoplasts (Fig. 3A, Supplemental Table S3). These results indicate tissue-
201 specific translation of sORFs. The most prominent group of translatable sORFs consisted of CDS-
202 sORFs (305, 51%) (Fig. 3B). Interestingly, the translation of 36 sORFs located on lncRNAs was also
203 detected by our analysis. Approximately 60% of the translated sORFs (349 sORFs) contained
204 “strong” and “medium” Kozak elements, which is a similar to the results obtained for all predicted
205 sORFs (~60%). This result suggests that translation initiation may differ for sORFs and protein
206 coding ORFs.

207 The length of translatable sORFs ranged from 11 to 100 amino acids (aa), which were generally
208 longer than untranslatable sORFs (Mann-Whitney *U* test $P = 4e-53$) (Fig. 3C). The length of
209 interlaced-sORFs differed significantly from that of CDS-sORFs and lncRNA-sORFs (Mann-Whitney *U*
210 test $P = 0.002$ and Mann-Whitney *U* test $P = 0.001$, respectively) but did not differ from uORFs
211 (Mann-Whitney *U* test $P = 0.06$). We observed that PSMs supporting SEP identifications had lower
212 average quality than those mapped to the protein sequences of all datasets (Supplemental Figs. S6A
213 and S6B). This finding is in agreement with data obtained for the animal kingdom (Slavoff et al. 2013;
214 Mackowiak et al. 2015). The quality of spectra and the values of PSMs supporting the expression of
215 SEPs were better in the “peptidomic” dataset (Supplemental Fig. S6C). Also, translatable sORFs were
216 longer for those identified in the peptidomic dataset (Supplemental Fig. S6D).

217 There were no significant dependencies between the level of expression of a transcript and
218 the chance of finding peptides from sORFs located on this transcript (logistic regression, P -value >>

219 0.05). However, among the 16 sORFs with evidence of translation in all types of moss cells, lncRNA-
220 sORFs were significantly overrepresented (Fisher's exact test, P-value = 0.001). Two of these SEPs,
221 Pp3c9_sORF1544 (41aa) and Pp3c25_sORF1000 (61aa), were common to all three cell types and
222 were confirmed by 15 and 17 unique endogenous peptides, respectively (Fig. 3D). The level of
223 transcription of some lncRNAs (according to the previous data (Fesenko et al. 2017) and evidences of
224 translation for the corresponding lncRNA-sORFs are shown in Fig. 3D. These data may point to
225 biological significance for the peptides translated from these sORFs rather than the sORFs having
226 regulatory functions in the translation of the main ORF. To explore this notion, we investigated the
227 functions of three SEPs encoded by lncRNAs (see below).

228 **sORFs can be translated together with proteins**

229 Several reports provide evidence that eukaryotic mRNA can have more than one coding ORF (bi- and
230 polycistronic genes) in both plants and animals (Blumenthal 1998; Rohrig et al. 2002; Pi et al. 2009;
231 Tautz 2009; Xu et al. 2010). Based on our MS data, we identified 144 loci with at least two translated
232 ORFs (annotated as main ORF and sORF), including 82 CDS-sORFs, that represent putative multi-
233 coding genes (Supplemental Table S4). The translation of multiple ORFs can occur from either
234 different transcripts of the same gene or consecutively from the single transcript (polycistronic
235 transcript). Some of the putative multi-coding genes were translated simultaneously with protein-
236 coding ORFs in the same type of moss cell (Fig. 3E), while others showed patterns of sORF and main
237 ORF translation such that their products were present in different types of cells (Fig. 3F). This
238 observation suggests that specific regulatory mechanisms may exist to fine-tune the translation of
239 both sORFs and proteins situated in the same gene locus. Taken together, our findings indicate that
240 at least 27% of translatable CDS-sORFs are expressed simultaneously with main ORFs and the
241 translation of sORFs and proteins located together in the same locus might be regulated in a tissue-
242 specific manner.

243

244 **Most translatable sORFs are not evolutionarily conserved**

245 Analysis of the evolutionary conservation of sORFs is often a key step in revealing biologically active
246 sORFs (Andrews and Rothnagel 2014). To determine whether the translatable sORFs were more
247 highly conserved than the other sORFs, we analyzed the intactness of these sORFs in the
248 reconstructed genomes of three *P. patens* ecotypes, 'Villersexel', 'Reute' and 'Kaskasia', as well as the
249 ten abovementioned species. We found that 19 (3.3%) of 584 translatable sORFs in the ecotypes
250 either lost the start/stop codon or had a frameshift or premature termination codon (PTC). This
251 number was not significantly different from the number (2.4%, 1598 sORFs) for which translation
252 was not detected by MS data, suggesting that sORF translation does not disrupt trends of sORF
253 elimination in these ecotypes.

254 To investigate whether the trend in translatable sORF evolution differs from that of the other sORFs,
255 we estimated the number of species in which homologs can be found and the selection pressure
256 (K_A/K_S) on translatable sORFs on an evolutionary timescale using the transcriptomes of the ten
257 abovementioned species. Overall, we found 73 sORFs had evidence of translation and conservation in
258 at least one species while only 11 were under negative selection ($K_A/K_S \ll 1$) (Supplemental Fig. S7).
259 Sixty-four (88%) of these were CDS-sORFs or interlaced-sORFs. These results suggest that these
260 types of sORFs are more conserved. Although conservative sORFs were significantly enriched in a set
261 of translatable sORFs (Fisher's exact test, $P = 2.716567e-05$), we found that most translatable sORFs
262 (87.6%) were not conserved.

263 We next examined whether the translatable sORFs detected in this study share similarity
264 with a recently defined set of 13,748 putative SEPs in the *A. thaliana* (Hazarika et al. 2017). We
265 identified two sORFs (Pp3c20_sORF627 (CDS-sORF), Pp3c11_sORF854 (CDS-sORF)) with evidence of
266 translation according to our MS analysis that shared similarity with ARA-PEP peptides (e -value <
267 0.01), implying that these sORFs are evolutionarily conserved and may produce peptides in *A.*
268 *thaliana* cells.

269

270 **Alternative splicing regulates the number of sORFs in protein-coding transcripts**

271 Alternative splicing (AS) events may lead to the specific gain, loss or truncation of different groups of
272 sORFs located on the transcripts of the same gene. For example, AS can generate sORFs that are
273 truncated version of proteins (see below). We found 6092 alternatively spliced sORFs (AS-sORFs)
274 belonging to transcripts from 4389 genes. CDS-sORFs were significantly overrepresented (Fig. 4A),
275 while interlaced-sORFs, uORFs and dORFs were significantly underrepresented among AS-sORFs
276 compared to the control dataset (AS-REF). The number of translatable sORFs in the set of AS-sORFs
277 did not significantly differ from that expected by chance (Fisher's exact test p-value=0.9423),
278 suggesting that AS does not preferentially occur in peptide-encoding sORFs. Ten GO terms linked
279 with nucleic acid binding (GO:0001071, GO:0003700), signal transducer activity (GO:0004871),
280 aminopeptidase activity (GO:0004177), transferase activity (GO:0003950, GO:0016772,
281 GO:0016775) and kinase activity (GO:0004672, GO:0004673, GO:0000155) were specifically
282 enriched in a set of AS-sORF-carrying genes. These results demonstrate that AS-sORFs are located in
283 regulatory genes more frequently than is expected by chance suggesting a potential role for sORFs in
284 the translational regulation of these genes.

285 We randomly selected ten different translatable AS-sORFs and searched for the
286 corresponding isoforms with/without sORFs in the transcriptomes of three types of moss cells. RT-
287 PCR analysis revealed the transcription of these isoforms, confirming that they could indeed be
288 translated (Supplemental Fig. S8). Moreover, four sORFs contained isoforms showing tissue-specific
289 transcription. These observations led to the hypothesis that the translation of sORFs is regulated by
290 AS.

291 We then classified the splicing events that lead to changes in sORF sequences into four
292 groups: 1) truncation, when the middle region of the sORF was excised by splicing; 2) stop codon
293 excision, when the sORF stop codon was spliced out; 3) start codon excision, when the sORF start
294 codon was spliced out; and 4) excision, if the complete sORF was removed from an isoform. We
295 found that half of the sORFs (48%, 2933) had undergone complete excision from their transcripts,
296 whereas only 93 sORFs were truncated (1.5%) and 517 sORFs (12%) were affected by two or more
297 events (Fig. 4B). Moreover, the complete excision of sORFs occurred significantly more frequently in

298 uORFs than in the other sORF groups (57% vs. 20–44%, Fisher’s exact test P-value < 1e-05). In
299 addition, evolutionarily conserved sORFs (conserved in >1 species) were significantly
300 underrepresented in the set of AS-sORFs that were subject to complete excision (Fisher’s exact test
301 P-value = 6.76e-42) compared to the other sets of AS-sORFs (“truncation”, “stop codon excision”, and
302 “start codon excision”). Thus, our analysis demonstrated that AS leads to the excision of sORFs from
303 the transcriptome of *P. patens*, preventing AS-sORF translation.

304

305 **The role of sORFs in modulating protein–protein interactions**

306 Protein–protein interactions (PPI) are critical for the formation of higher order protein complexes.
307 Competitive inhibitors of PPI are referred to as MicroProteins (miPs) or small interfering peptides
308 (siPEPs) (Seo et al. 2011; Eguen et al. 2015). These proteins, which are usually small, can be
309 generated by alternative splicing or evolutionarily generated by domain loss (Staudt and Wenkel
310 2011; Eguen et al. 2015). We hypothesized that sORFs with similarity to known proteins may
311 compete with such proteins to impair their functions. To identify such sORFs, we performed BLASTP
312 (E-value < e-5) similarity searches between the encoded amino acid sequences of sORFs and the
313 annotated proteins of *P. patens*. We identified 363 sORFs resulting from AS events that partially
314 overlapped with the main ORF, thereby generating truncated versions of the proteins. Based on the
315 analogy of cis-miPs generated by alternative splicing events (Eguen et al. 2015), we will refer to
316 these SEPs as cis-SEPs (and accordingly, cis-sORFs; Supplemental Table S5).

317 We analyzed how many cis-ORFs contained known complete or incomplete protein domains, finding
318 that 60 sORFs harbored intrinsically disordered regions (IDRs, (van der Lee et al. 2014)), while 30
319 cis-sORFs contained parts of 28 different domains (Supplemental Table S5). The genes containing
320 cis-sORFs were enriched in kinase and kinase-like domains. Among these, we observed the protein
321 kinase domain (PS50011, Pp3c13_sORF653), protein tyrosine kinase (PF07714, Pp3c11_sORF2084)
322 and MYB-like DNA-binding domain (TIGR01557, Pp3c19_sORF797). GO enrichment analysis also
323 revealed significant overrepresentation of terms associated with protein modifications, such as
324 GO:0006468 (protein phosphorylation) and GO:0036211 (protein modification process).

325 Among genes containing cis-sORFs, we identified some with similarity to putative transcription factor
326 genes (TFs) such as genes encoding GROWTH-REGULATING FACTOR (e.g., Pp3c20_10590), C2H2
327 zinc finger domain containing (e.g., Pp3c1_16920), BTB/POZ domain containing (e.g., Pp3c16_9230), B3
328 DNA binding domain containing (e.g., Pp3c7_7990) and MYB-CC type transcription factor (e.g.,
329 Pp3c21_2850). Due to their similarity with TF domains, we predict they may act as dominant-negative
330 repressors of TFs.

331 To obtain evidence for the translation of these sORFs, we analyzed MS data and found at least
332 two examples (Fig. 4C). A few detected translatable cis-sORFs could be explained by a significant
333 overlap with the protein sequences, whereas we filtered out the 'ambiguous' PSMs. Moreover, the
334 formation of a premature termination codon (PTC) as a result of intron retention events, might lead
335 to mRNA decay (Ge and Porse 2014; Karousis et al. 2016) and rapid nonsense-mediated decay
336 (NMD)-coupled degradation of sORF-encoded peptides (Popp and Maquat 2013).

337 We identified 272 sORFs that shared similarity with annotated proteins but were located on
338 other transcripts (trans-sORFs, see in Supplemental Table S5). The translation of six trans-sORFs was
339 confirmed by our MS data. We found 36 potential trans-SEPs with similarity to known protein
340 domains (Supplemental Table S5). Trans-sORFs may have originated through the divergence of
341 ancient paralogous genes, which occurred after the paleo duplication of the moss genome (Rensing et
342 al. 2007; Rensing et al. 2008). In fact, 159 (58.5%) trans-sORFs shared similarity to genes from at
343 least one species. In addition, all of these trans-sORFs are under strong purifying selection ($K_A/K_S \ll$
344 1).

345 We then investigated which trans-sORFs share similarity to large gene families. Several
346 distinct clusters with sORF-encoded peptides sharing similarity with more than four proteins from
347 distinct genes were detected (Supplemental Fig. S9). Each cluster encompasses genes from different
348 protein families, including one containing leucine-rich repeat and zinc-finger domains involved in
349 protein-protein and protein-nucleic acid interactions, respectively.

350 To compete with target proteins, we presume that potential SEPs and their targets should
351 coexist in a cell. We examined the co-expression data and compared the distribution of correlation
352 coefficient values with those from randomly selected pairs (10 iterations) of genes. On average, these

353 sORF-protein pairs had higher correlation coefficients than randomly selected gene pairs (Wilcoxon
354 Rank Sum and Kolmogorov-Smirnov Tests P-value < 0.05), implying that sORF-bearing and target
355 genes are frequently co-expressed.

356 **SEPs regulate moss growth**

357 Despite the recent finding that 10% of overexpressed intergenic sORFs have clear phenotypes in
358 Arabidopsis (Hanada et al. 2013), the functions of most sORFs and SEPs in plants are generally
359 unknown. Known bioactive SEPs in plants are encoded by sORFs located on short non-protein-coding
360 transcripts, which can be referred to as lncRNAs (Rohrig et al. 2002; Chilly et al. 2006). In this
361 context, it would be intriguing to determine how many plant lncRNAs encode peptides, as well as the
362 biological functions of these SEPs. Our pipeline allowed us to identify hundreds of translated sORFs,
363 including those encoded by lncRNAs. Some of these lncRNA-sORFs showed tissue-specific
364 transcription and translation patterns, while others were expressed in all types of moss cells (Fig.
365 3C). We reasoned that stably expressed lncRNA-sORFs can produce peptides that play fundamental
366 roles in various cellular processes. To explore this hypothesis, we examined the impact of lncRNA-
367 sORF overexpression and knockout on moss morphology using three conserved lncRNAs-sORFs:
368 Pp3c9_sORF1544, Pp3c25_sORF1253, Pp3c25_sORF1000 (Fig. 3C). We obtained multiple
369 independent mutant lines for each of these lncRNAs-sORFs (Supplemental Figs. S10 and S11). Both
370 the overexpression and knockout of sORFs resulted in morphological changes, implying that these
371 peptides play a role in growth and development of *P. patens* (Fig. 5).

372 Overexpression of a 41-aa peptide (*PSEP1*, *Physcomitrella patens* sORF encoded peptide 1) encoded
373 by the lncRNA-sORF Pp3c9_sORF1544 resulted in longer caulonema cells (filaments implicated in a
374 rapid radial extension of the protonemal tissues) compared to the wild-type and knockout lines (Figs
375 5A-G, Supplemental Fig. S12). Moreover, there was a significant difference in growth rate between
376 the wild-type and *psep1* mutant lines (Fig. 5G). Rapid growth in the *PSEP1* overexpressing lines was
377 accompanied by earlier aging and cell death (Supplemental Fig. S13).

378 The lines with a knockout in a 57-aa peptide (*PSEP3*), encoded by lncRNA-sORF Pp3c25_sORF1253
379 displayed a decrease in growth rate, altered filament branching, and shorter lateral filaments
380 compared to the wild type (Figs. 5H-L, Supplemental Fig. S12). Similar to the results for the *PSEP3*

381 knockout, knocking out a 61-aa peptide (*PSEP25*) encoded by lncRNA-sORF Pp3c25_sORF1000 also
382 resulted in a decreased in growth rate and altered protonemal architecture on cultural medium
383 without glucose (Figs. 50-T). *PSEP25* knockouts also had an increase in the number of leafy shoots
384 (Figs. 5Q, R and T).

385 Taken together, our findings suggest that lncRNA-sORFs can influence growth and
386 development in moss.

387 DISCUSSION

388 Although functionally characterized SEPs have been shown to play fundamental roles in key
389 physiological processes, sORFs are arbitrarily excluded during genome annotation. Given the
390 difficulty in identifying translatable, functional sORFs, we know little about their origin, evolution
391 and regulation in the genome. In the present study, we investigated the abundance, evolutionary
392 history and possible functions of sORFs in the genome of the model moss *Physcomitrella patens*. The
393 use of an integrated pipeline that includes transcriptomics, proteomics, and peptidomics data
394 allowed us to identify hundreds of translatable sORFs in three types of moss cells. We propose that
395 several distinct classes of sORFs that differ in terms of their position on transcripts, the level of
396 evolutionary conservation, and possible functions are present in the moss genome (Fig. 6).

397 sORFs with high coding potential are not conserved among genomes

398 Even though the analysis of sequence conservation is somewhat biased against the detection of short
399 sequences (Ladoukakis et al. 2011), this technique is widely used to select candidate functional
400 sORFs. Although analyzing the conservation of short amino acid sequences is not trivial (Moyers and
401 Zhang 2016), hundreds of conserved sORFs have recently been identified in plants, yeast and
402 animals (Ladoukakis et al. 2011; Hanada et al. 2013; Mackowiak et al. 2015). The number of sORFs
403 conserved in the plant kingdom is undoubtedly underestimated due to the low sensitivity of tools
404 used for conservation analysis and the limited number of available sequenced genomes from closely
405 related species. Our pipeline allowed us to identify 5034 conserved sORFs among the transcriptomes
406 of ten different plant species, 71 of which showed evidence of translation according to our MS data.

407 However, we suggest that the possibly functional sORFs might significantly outnumber the
408 conserved ones.

409 Despite the evidence for translation of approximately 1% of uORFs and dORFs, these sORF
410 types were significantly underrepresented among the sORFs that are conserved in the closest related
411 species. We even detected rapid inactivation of uORFs and dORFs in the reconstructed genomes of
412 three *P. patens* ecotypes due to disruptions in the start or stop codons (47% of the total disrupted
413 sORFs). As the occurrence of sORFs downstream or upstream of the main ORF can be deleterious to
414 its translation, we cannot rule out the possibility that this may cause strong selection pressure and
415 the rapid elimination of uORFs and dORFs (Iacono et al. 2005; Neafsey and Galagan 2007; Johnstone
416 et al. 2016). Moreover, we observed significant depletion (Fisher's exact test P-value = 5.25e-13) of
417 uORFs and dORFs in a set of translatable conservative sORFs. Taken together, these findings suggest
418 that sORFs located in untranslated regions are evolving rapidly and may play regulatory roles rather
419 than encoding bioactive peptides.

420 In recent studies, thousands of alternative proteins were experimentally detected in human
421 cell lines (Vanderperre et al. 2013; Samandi et al. 2017). In *P. patens*, we found tens of thousands of
422 sORFs (CDS-sORFs) that overlapped with the CDS of protein-coding genes, 305 of which were
423 translatable. The evolution of CDS-sORFs is undoubtedly an expensive process for the cell, as these
424 elements may be located in regions encoding protein domains and influence the structure and
425 function of the protein encoded by the main ORF (Cherry 2010). We found both CDS-sORFs
426 originated from regions associated with known protein domains and CDS-sORFs from disordered
427 regions, with higher conservation for CDS-sORFs originated from protein domain-encoding regions.
428 These results indicate that the evolution of CDS-sORFs depends on their locations insight main CDS
429 sequence.

430 In the current study, we found that both the transcription and translation of CDS-sORFs
431 occurred in a tissue-specific manner. Protein-coding genes with tissue-specific transcription patterns
432 and functional redundancy of the gene product are often under positive selection (Zhang and Li
433 2004; Montoya-Burgos 2011). This finding, together with other properties of CDS-sORFs, such as
434 their overlap with particular parts of protein-coding sequences, might explain the high turnover rate

435 of CDS-sORFs. However, whether sORFs are preferentially generated in fast-evolving regions of
436 proteins or whether the selective pressure on sORFs leads to changes in protein-coding sequences is
437 still unknown.

438 **Analysis of sORF translation: approaches that makes sense**

439 It was recently suggested that sORFs are randomly generated in a genome (Couso and Patraquim
440 2017). Assuming that the average length of an sORF is approximately 60 bp and that sORFs do not
441 overlap, these elements occupy a substantial portion of the moss genome. This raises the question: to
442 what extent are sORFs present in the transcriptome and the proteome of a cell? According to
443 ribosome profiling data from a wide variety of species, sORFs translation appears to occur in a
444 pervasive manner (Ingolia et al. 2011; Guttman et al. 2013; Bazzini et al. 2014; Couso and Patraquim
445 2017). However, ribosome-profiling data alone are not sufficient to classify transcripts as coding or
446 noncoding (Guttman et al. 2013). Thus, alternative approaches such as proteomics and peptidomics
447 should be used to investigate the translation of sORFs (Slavoff et al. 2013; Ma et al. 2016). Mass-
448 spectrometry studies have thus far confirmed the presence of a few dozen SEPs in the peptidomes of
449 animal cells (Slavoff et al. 2013; Prabakaran et al. 2014; Mackowiak et al. 2015; Ma et al. 2016).
450 Comparisons of ribosome profiling and mass spectrometry results have led to the conclusion that MS
451 detects peptides arising from the most highly translated sORFs (Aspden et al. 2014; Bazzini et al.
452 2014). However, a recent study showed that there are no technical obstacles to the detection of
453 sORF-encoded peptides by mass spectrometry (Verheggen et al. 2017).

454 In previous studies, only standard proteomics analysis was used to identify SEPs. We
455 reasoned that analyzing endogenous peptide pools instead of tryptic peptides has several
456 disadvantages in terms of SEP identification: 1) standard proteomic approaches are not suitable for
457 the isolation and analysis of small and low-abundance peptide molecules; and 2) SEPs are shorter
458 than standard proteins and it is unlikely that more than one tryptic fragment will be detected in a
459 single proteomic experiment. Moreover, peptidomic approaches can theoretically be used to identify
460 full-length SEPs in a cell. We firstly used endogenous peptides pools to detect SEPs and according to
461 our data the values of PSMs, supporting expression of SEPs, were better in “peptidomic” dataset.
462 Moreover, some SEPs were confirmed by several endogenous peptides (up to 17), that an increase

463 the reliability of their detection. Notably, we did not observe any significant overlap between the
464 sORFs detected using proteomic and peptidomic approaches. Thus, our study demonstrates the
465 advantage of using complementary approaches for building a complete list of SEPs.

466 According to our MS data, the translation patterns of most sORFs tend to be tissue specific
467 (Fig. 3A). We suggest that the slight overlap in tissue-specific expression among SEPs from various
468 types of moss cells could be due to either specific SEP post-translational modification (PTM)
469 patterns, tissue-specific transcription of sORFs, or the limitations of mass-spectrometry in detecting
470 low-abundance or modified sORF-encoded peptides. According to our results, alternative splicing is
471 an additional mechanism that control tissue-specific sORF expression in plant cells. Also, the number
472 of sORFs that were commonly translated between two types of moss cells was higher for related cell
473 types: protonemata and gametophores (two growth stages) as well as protonemata and protoplasts
474 (protoplasts were generated from the protonemata). These observations indicate tissue-specific
475 characteristics of SEPs translation and modification rather than technical limitation in detection.

476 **Functionality of SEPs**

477 We identified hundreds of translatable sORFs representing multiple sORF types and suggested
478 various functions for the types of sORFs (Fig. 6). Clear evidence of transcription and translation
479 points to a possible biological significance of the sORFs that we identified here. Based on our
480 conservation analysis and MS data, we suggest that the majority of uORFs and dORFs play regulatory
481 roles instead of encoding peptides (Fig. 6A). By contrast, CDS-, interlaced- and lncRNA-sORFs have
482 greater potential to encode bioactive peptides, as they are more highly conserved, frequently contain
483 known protein domains and, according to the MS data, often produce peptides. However, the
484 functions of these peptides are unclear and require more detailed investigation.

485 One possible role for sORF-encoded peptides that are similar to known proteins is to mimic the
486 similar protein to interfere with its function. MiPs (or siPEPs) are important modulators of protein-
487 protein and protein-DNA interactions that, for example, prevent the formation of functional protein
488 complexes (Seo et al. 2013; Graeff et al. 2016). We suggest that the potential for sORFs that overlap
489 with the CDS of protein-coding genes to be a source of small interfering peptides is currently
490 underestimated (Fig. 6B). We found that approximately 30% of cis-SEPs harbor protein domains

491 such as protein kinase domains and MYB-like DNA-binding domain or IDRs. The genes harboring
492 CDS-sORFs were enriched in GO terms connected to protein binding and transferase activity. Also,
493 some sORFs with disordered regions might mediate protein-protein or protein-nucleic acid
494 interactions, as suggested previously (Mackowiak et al. 2015). Taken together, these findings suggest
495 that sORFs may strongly interfere with protein interactions.

496 In this study, we explored several groups of sORFs, including those encoded by lncRNAs. The
497 translation of peptides from lncRNAs is intriguing, and there is some evidence that these peptides
498 play important biological roles in various processes (Kondo et al. 2010; Magny et al. 2013;
499 Matsumoto et al. 2017). Nevertheless, the biological functions of most lncRNA-sORF-encoded
500 peptides are currently unclear, especially those in the plant kingdom (Tavormina et al. 2015).

501 The transcription of the non-coding portions of the genome into lncRNAs is thought to give
502 rise to the translation of sORFs located within them. In this case, some of these peptides would not be
503 vital but may be important for survival under certain conditions by serving as a raw material for
504 evolution (Fig. 6C). Knocking out select lncRNA-encoded peptides was not lethal in moss, but did
505 influence moss growth under certain conditions. On the other hand, plants overexpressing an
506 lncRNA-encoded peptide (41 aa) showed phenotypic differences compared to wild-type plants,
507 suggesting a possible role for the lncRNA-encoded peptide in regulating cell growth and
508 development. Our results lay the groundwork for systematic analysis of functional peptides encoded
509 by sORFs.

510 The possible evolution of non-coding portions of the genome into protein-coding genes is
511 also a subject of intensive debate (Carvunis et al. 2012; McLysaght and Guerzoni 2015; Couso and
512 Patraquim 2017). According to our data, putative homologous sORFs tended to differ in length in
513 most cases (Fig. 2D). Thus, we suggest that most sORFs expanded during evolution, providing
514 support for the notion that they function as raw materials for selection; however, this point requires
515 further confirmation.

516

METHODS

517 ***Physcomitrella patens* growth conditions**

518 *Physcomitrella patens* protonemata were grown on BCD medium supplemented with 5 mM
519 ammonium tartrate (BCDAT) or 0.5% glucose during a 16-h photoperiod at 25°C in 9-cm Petri dishes
520 (Nishiyama et al. 2000). For all analyses, the protonemata were collected every 5 days. The
521 gametophores were grown on free-ammonium tartrate BCD medium under the same conditions, and
522 8-week-old gametophores were used for analysis. Protoplast was prepared from protonemata as
523 described previously (Fesenko et al. 2015).

524 For morphological analysis, protonemal tissue 2 mm in diameter were inoculated on BCD and
525 BCDAT 9-cm Petri dishes. For growth rate measurements, photographs were taken at 7 d intervals
526 over 42 days. Protonemal tissues and cells were photographed using a Microscope Digital Eyepiece
527 DCM-510 attached to a Stemi 305 stereomicroscope or Olympus CKX41.

528

529 **Identification of coding sORFs in the *P. patens* genome**

530 To identify sORFs with high coding potential, the sORFinder (Hanada et al. 2010) tool was utilized.
531 Intron sequences and CDS were used as negative and positive sets, respectively. Additional details
532 are described in the Supplemental Methods. To select for sORFs that are transcribed, located in the
533 exons of transcripts, and have introns, a bed file was generated using a python script (GffParser.py)
534 and intersected with exon positions extracted from a gff3 file of *P. patens* genome annotations. To
535 identify intergenic-sORFs, the bed file was also intersected with transcribed regions determined
536 based on our RNAseq data (Fesenko et al. 2017). Using an R script, sORFs fully overlapping with
537 exons were selected; 75,685 sORFs remained after this step. Identical sORFs were removed from the
538 dataset. In addition, sORFs overlapping repetitive regions identified by RepeatMasker, as well as
539 sORFs comprising parts of annotated *P. patens* proteins, were also removed from the dataset,
540 resulting in a final dataset of sORFs comprising 70,095 sequences.

541

542 **sORF classification**

543 The step-by-step procedure performed for sORF classification is illustrated in Supplemental Fig. S14.
544 In the first step, lncRNA-sORFs were identified by searching for identical sORFs in known lncRNA
545 databases, including CantataDB (Szczesniak et al. 2016), GreenC (Paytuyi Gallart et al. 2016) and our
546 previously published moss dataset (Fesenko et al. 2017). After this sORF bed file was intersected
547 with moss genome annotation, the locations of the sORFs on transcripts were determined, resulting
548 in the further classification of genic-sORFs into uORFs, dORFs, CDS-sORFs and interlaced-sORFs.

549 Because alternative splicing leads to inaccuracy in genome annotation, the locations of a
550 subset of genic-sORFs cannot be unambiguously classified, as they can be located in different regions
551 in different isoforms of the same gene. All sORFs located on transcripts that were not annotated in
552 the *P. patens* genome but were identified using our RNAseq data were classified as intergenic-sORFs.

553 To detect alternatively spliced sORFs (AS-sORFs), a bed file with sORF locations was
554 intersected with a bed file containing intron coordinates for all isoforms. Those sORFs that
555 overlapped for both exons (see above) and introns were classified as AS-sORFs.

556

557 **Evolutionary conservation analysis**

558 The transcriptomes of nine plant species were downloaded from Phytozome v12: *Sphagnum fallax*
559 (release 0.5), *Marchantia polymorpha* (release 3.1), *Selaginella moellendorffii* (release 1.0), *Spirodela*
560 *polyrhiza* (release 2), *Arabidopsis thaliana* (TAIR 10), *Zea mays* (Ensembl-18), *Oryza sativa* (release
561 7), *Volvox carteri* (release 2.1) and *Chlamydomonas reinhardtii* (release 5.5). The transcriptome of
562 *Ceratodon purpureus* was *de novo* assembled using Trinity (Haas et al. (2013)). To identify
563 transcribed homologous sequences, tBLASTn (word size = 3) was performed using sORF peptide
564 sequences as queries and the transcriptome sequences of the abovementioned species as subjects.
565 The following cutoffs parameters were used to distinguish reliable alignments: E-value < e-5 and
566 query coverage > 60%. Our E-value cutoff was obtained by applying a multiple comparison
567 correction (Bonferroni correction) of 0.05, which is commonly used in biological experiments.

568 Pairwise K_A/K_S ratios were calculated using the codeml algorithm with PAML software (Yang
569 2007). The calculation procedure, which was facilitated using a custom-made python script

570 (protein_Ka_Ks_codeml.py), included alignment extraction from the tBLASTn output, PAL2NAL
571 (Suyama et al. 2006) correction of the nucleotide alignment using the corresponding aligned protein
572 sequences and calculation of K_A/K_S ratios using codeml. The script implements packages from
573 biopython (Cock et al. 2009). To estimate homologous sORF lengths, a python script
574 (sORF_completeness_v2.0.py) was designed. Additional details are described in the Supplemental
575 Methods.

576 **GO enrichment analysis**

577 GO enrichment analysis was performed using the topGO bioconductor R package using the Fisher's
578 exact test in conjunction with the 'classic' algorithm (false discovery rate [FDR] < 0.05). Gene
579 Ontology (GO) terms assigned to *P. patens* genes were downloaded from Phytozome. Only GO terms
580 containing >5 genes in a background dataset were considered in the enrichment analysis. Redundant
581 GO terms were removed using the web-based tool REVIGO (Supek et al. 2011).

582

583 **Peptide and protein extraction**

584 Endogenous peptide extraction was conducted as described previously (Fesenko et al. 2015). Proteins were
585 extracted as described previously (Fesenko et al. 2016). Additional details are described in the
586 Supplemental Methods.

587 **Mass-spectrometry analysis and peptide identification**

588 Mass-spectrometry analysis was performed using three biological and three technical repeats for the
589 proteomic (Fesenko et al. 2017) and peptidomic datasets. Analysis was performed on two different
590 mass spectrometers: a TripleTOF 5600+ mass spectrometer with a NanoSpray III ion source
591 (ABSciex, Canada) and a Q Exactive HF mass spectrometer (Q Exactive HF Hybrid Quadrupole-
592 Orbitrap mass spectrometer, Thermo Fisher Scientific, USA). Additional details are described in the
593 Supplemental Methods.

594 All datasets were searched individually with MaxQuant v1.5.8.3 (Tyanova et al. 2016) against
595 a custom database containing 32926 proteins from annotated genes in the latest version of the moss
596 genome (V3.1, (Lang et al. 2018)), 85 moss chloroplast proteins, 42 moss mitochondrial proteins and

597 72095 predicted sORF peptides. MaxQuant's protein FDR filter was disabled, while 1% FDR was used
598 to select high-confidence PSMs, and ambiguous peptides were filtered out. Moreover, any PSMs with
599 Andromeda scores of less than 30 were discarded (to exclude poor MS/MS spectra). For the dataset
600 of endogenous peptides (named "peptidomic", Supplementary Table S2), the parameter "Digestion
601 Mode" was set to "unspecific" and modifications were not permitted. All other parameters were left
602 as default values. For the dataset of tryptic peptides (named "proteomic") the parameter "Digestion
603 Mode" was set to "specific" (the Trypsin/P), MaxQuant's protein FDR filter was disabled, and the
604 peptide FDR remained at 1%. All other parameters were left as default values. Features of the PSMs
605 (length, intensity, number of spectra, Andromeda score, intensity coverage and peak coverage) were
606 extracted from MaxQuant's msms.txt files.

607 To filter out MS peptides that do not provide unambiguous evidence of sORF peptide
608 expression, we assessed the number of times a peptide occurred in the whole moss genome by
609 searching for exact matches to the MS peptides in the six-frame translated genome. Of 629 unique
610 peptides, 595 peptides (corresponding to 570 sORFs) matched only to the corresponding sORF
611 peptide in the translated genome. The moss genome has a number of paralogous genes that resulted
612 from two whole-genome duplication events (Lang et al. 2018). MS peptides from such paralogous
613 sORFs will be discarded if they match to more than one locus in the genome. To prevent this, we
614 identified paralogous sORFs in the moss genome by tBLASTn and aligned their coordinates with the
615 multi-hit MS peptide coordinates. This identified 15 MS peptides (14 sORFs) that matched to
616 paralogous sequences and were discarded from further analysis. Our final high-confidence set
617 included 584 translatable sORFs.

618 **RT-PCR analysis of AS-sORFs**

619 Total RNA from gametophores, protonema and protoplasts was isolated as previously described
620 (Cove et al. 2009). RNA quality and quantity were evaluated via electrophoresis in an agarose gel
621 with ethidium bromide staining. The precise concentration of total RNA in each sample was
622 measured using a Quant-iT™ RNA Assay Kit, 5–100 ng on a Qubit 3.0 (Invitrogen, US) fluorometer.
623 The cDNA for RT-PCR was synthesized using an MMLV RT Kit (Evrogen, Russia) according to the
624 manufacturer's recommendations employing oligo(dT)₁₇-primers from 2 µg total RNA after DNase

625 treatment. The primers were designed using Primer-BLAST (Ye et al. 2012) (Supplementary Table).
626 The minus reverse transcriptase control (-RT) contained RNA without reverse transcriptase
627 treatment to confirm the absence of DNA in the samples. The RT-PCR products were resolved on an
628 1.5% agarose gel and visualized using ethidium bromide staining.

629 **Generation of overexpression and knockout lines**

630 To obtain overexpression lines of the PSEP1 (Pp3c9_sORF1544), PCR was carried out using genomic
631 DNA as a template and PEP4f and PEP4r primers (Supplemental Table S6). Amplicons were cloned
632 into the pPLV27 vector (GenBank JF909480) using the Ligation-independent (LIC) procedure
633 (Aslanidis and de Jong 1990; De Rybel et al. 2011). The resulting plasmid was named pPLV-Hpa-4FR
634 and used for transformation. Additional details are described in the Supplemental Methods.

635 PSEP1 (sORF Pp3c9_sORF1544), PSEP3 (Pp3c25_sORF1253) and PSEP25
636 (Pp3c25_sORF1000) knockout lines were created using the CRISPR-Cas9 system (Collonnier et al.
637 2017). The coding sequences were used to search for CRISPR RNA (crRNA) preceded by a *S. pyogenes*
638 Cas9 PAM motif (NGG) using the web tool CRISPR DESIGN (<http://crispr.mit.edu/>). The crRNA
639 closest to the translation start site (ATG) was selected for cloning (Supplemental Table S6).

640 Protoplasts were transformed using PEG transformation protocol (Schaefer and Zryd 1997).
641 Additional details are described in the Supplemental Methods. The plasmids pACT-CAS9 (for CAS9
642 expression) and pBNRF (resistance to G418) were kindly provided by Dr. Fabien Nogué.

643 Independent knockout and overexpression mutant lines have been obtained (Supplemental
644 Figs. S10-12).

645 The ploidy level of the *PSEP1* overexpression and *psep1* knock-out lines were estimated using
646 flow cytometry. Protoplasts were fixed in cold 70 % methanol, washed in TBS with 0.1 % Triton X-
647 100, then washed with TBS and stained with 500 ng/ml DAPI. The fluorescence was analyzed with a
648 flow cytometer NovoCyte (ACEA Biosciences) and Novoexpress data software. Fluorescence was
649 excited at 405 nm, and detection was at 445/45 nm.

650

651

652

653 **DATA ACCESS**

654 All raw mass spectrometry data from this study have been deposited to the ProteomeXchange
655 Consortium via the PRIDE (Vizcaino et al. 2016) partner repository with the dataset identifiers
656 PXD005223, PXD007922, PXD007923, PXD007973.

657

658 **SOFTWARE AVAILABILITY**

659 All data were analyzed using Python (<http://www.python.org>, v 3.5), and R ([http://www.R-](http://www.R-project.org)
660 [project.org](http://www.R-project.org), R Development Core Team 2006). All scripts are available at Zenodo (doi:
661 10.5281/zenodo.1160331) and are maintained in the GitHub code repository:
662 https://github.com/Kirovez/Scripts_sORFs_MS.

663

664 **ACKNOWLEDGEMENTS**

665 This work was supported by the Russian Science Foundation (project No.17-14-01189). Some of mass
666 spectrometric measurements were performed using the equipment of the “Human Proteome” Core
667 Facility of the Orekhovich Institute of Biomedical Chemistry (Russia) which is supported by the
668 Ministry of Education and Science of the Russian Federation.

669 **Authors' contributions**

670 IF and IK conceived and designed experiments. AK performed moss transformation experiments.
671 IF, RK, VL, DK, EG, VZ, IB and AM performed the proteomics analyses. IF, IK and GA performed the
672 statistical and bioinformatics analyses. IF, IK, VI and VG wrote the manuscript with input from all
673 authors. IF supervised the project. All authors read and approved the final manuscript.

674 **DISCLOSURE DECLARATION**

675 The authors declare that they have no significant competing financial, professional, or personal
676 interests that might have influenced the performance or presentation of the work described in this
677 manuscript.

678

679 **REFERENCES**

680 Andrews SJ, Rothnagel JA. 2014. Emerging evidence for functional peptides encoded by short
681 open reading frames. *Nat Rev Genet* **15**(3): 193-204.

- 682 Aslanidis C, de Jong PJ. 1990. Ligation-independent cloning of PCR products (LIC-PCR).
683 *Nucleic acids research* **18**(20): 6069-6074.
- 684 Aspden JL, Eyre-Walker YC, Phillips RJ, Amin U, Mumtaz MA, Brocard M, Couso JP. 2014.
685 Extensive translation of small Open Reading Frames revealed by Poly-Ribo-Seq. *eLife*
686 **3**: e03528.
- 687 Bazzini AA, Johnstone TG, Christiano R, Mackowiak SD, Obermayer B, Fleming ES, Vejnar CE,
688 Lee MT, Rajewsky N, Walther TC et al. 2014. Identification of small ORFs in
689 vertebrates using ribosome footprinting and evolutionary conservation. *The EMBO*
690 *journal* **33**(9): 981-993.
- 691 Blanvillain R, Young B, Cai YM, Hecht V, Varoquaux F, Delorme V, Lancelin JM, Delseny M,
692 Gallois P. 2011. The Arabidopsis peptide kiss of death is an inducer of programmed
693 cell death. *The EMBO journal* **30**(6): 1173-1183.
- 694 Blumenthal T. 1998. Gene clusters and polycistronic transcription in eukaryotes. *BioEssays :*
695 *news and reviews in molecular, cellular and developmental biology* **20**(6): 480-487.
- 696 Carvunis AR, Rolland T, Wapinski I, Calderwood MA, Yildirim MA, Simonis N, Charlotteaux B,
697 Hidalgo CA, Barbette J, Santhanam B et al. 2012. Proto-genes and de novo gene birth.
698 *Nature* **487**(7407): 370-374.
- 699 Cherry JL. 2010. Expression level, evolutionary rate, and the cost of expression. *Genome*
700 *biology and evolution* **2**: 757-769.
- 701 Chillely PM, Casson SA, Tarkowski P, Hawkins N, Wang KL, Hussey PJ, Beale M, Ecker JR,
702 Sandberg GK, Lindsey K. 2006. The POLARIS peptide of Arabidopsis regulates auxin
703 transport and root growth via effects on ethylene signaling. *Plant Cell* **18**(11): 3058-
704 3072.
- 705 Cock PJ, Antao T, Chang JT, Chapman BA, Cox CJ, Dalke A, Friedberg I, Hamelryck T, Kauff F,
706 Wilczynski B et al. 2009. Biopython: freely available Python tools for computational
707 molecular biology and bioinformatics. *Bioinformatics* **25**(11): 1422-1423.
- 708 Collonnier C, Epert A, Mara K, Maclot F, Guyon-Debast A, Charlot F, White C, Schaefer DG,
709 Nogue F. 2017. CRISPR-Cas9-mediated efficient directed mutagenesis and RAD51-
710 dependent and RAD51-independent gene targeting in the moss *Physcomitrella*
711 *patens*. *Plant Biotechnol J* **15**(1): 122-131.
- 712 Couso JP. 2015. Finding smORFs: getting closer. *Genome Biol* **16**.
- 713 Couso JP, Patraquim P. 2017. Classification and function of small open reading frames.
714 *Nature reviews Molecular cell biology*.
- 715 Cove DJ, Perroud PF, Charron AJ, McDaniel SF, Khandelwal A, Quatrano RS. 2009. Isolation of
716 DNA, RNA, and protein from the moss *Physcomitrella patens* gametophytes. *Cold*
717 *Spring Harbor protocols* **2009**(2): pdb prot5146.
- 718 D'Lima NG, Ma J, Winkler L, Chu Q, Loh KH, Corpuz EO, Budnik BA, Lykke-Andersen J,
719 Saghatelian A, Slavoff SA. 2017. A human microprotein that interacts with the mRNA
720 decapping complex. *Nat Chem Biol* **13**(2): 174-180.
- 721 De Coninck B, Carron D, Tavormina P, Willem L, Craik DJ, Vos C, Thevissen K, Mathys J,
722 Cammue BP. 2013. Mining the genome of *Arabidopsis thaliana* as a basis for the
723 identification of novel bioactive peptides involved in oxidative stress tolerance. *J Exp*
724 *Bot* **64**(17): 5297-5307.
- 725 De Rybel B, van den Berg W, Lokerse A, Liao CY, van Mourik H, Moller B, Peris CL, Weijers D.
726 2011. A versatile set of ligation-independent cloning vectors for functional studies in
727 plants. *Plant Physiol* **156**(3): 1292-1299.
- 728 Djordjevic MA, Mohd-Radzman NA, Imin N. 2015. Small-peptide signals that control root
729 nodule number, development, and symbiosis. *J Exp Bot* **66**(17): 5171-5181.
- 730 Eguen T, Straub D, Graeff M, Wenkel S. 2015. MicroProteins: small size-big impact. *Trends*
731 *Plant Sci* **20**(8): 477-482.

- 732 Fesenko I, Khazigaleeva R, Kirov I, Kniazev A, Glushenko O, Babalyan K, Arapidi G, Shashkova
733 T, Butenko I, Zgoda V et al. 2017. Alternative splicing shapes transcriptome but not
734 proteome diversity in *Physcomitrella patens*. *Scientific reports* **7**(1): 2698.
- 735 Fesenko I, Seredina A, Arapidi G, Ptushenko V, Urban A, Butenko I, Kovalchuk S, Babalyan K,
736 Knyazev A, Khazigaleeva R et al. 2016. The *Physcomitrella patens* Chloroplast
737 Proteome Changes in Response to Protoplastation. *Front Plant Sci* **7**: 1661.
- 738 Fesenko IA, Arapidi GP, Skripnikov AY, Alexeev DG, Kostyukova ES, Manolov AI, Altukhov
739 IA, Khazigaleeva RA, Seredina AV, Kovalchuk SI et al. 2015. Specific pools of
740 endogenous peptides are present in gametophore, protonema, and protoplast cells of
741 the moss *Physcomitrella patens*. *Bmc Plant Biol* **15**: 87.
- 742 Ge Y, Porse BT. 2014. The functional consequences of intron retention: alternative splicing
743 coupled to NMD as a regulator of gene expression. *BioEssays : news and reviews in*
744 *molecular, cellular and developmental biology* **36**(3): 236-243.
- 745 Giannakakis A, Zhang J, Jenjaroenpun P, Nama S, Zainolabidin N, Aau MY, Yarmishyn AA, Vaz
746 C, Ivshina AV, Grinchuk OV et al. 2015. Contrasting expression patterns of coding and
747 noncoding parts of the human genome upon oxidative stress. *Scientific reports* **5**:
748 9737.
- 749 Graeff M, Straub D, Eguen T, Dolde U, Rodrigues V, Brandt R, Wenkel S. 2016. MicroProtein-
750 Mediated Recruitment of CONSTANS into a TOPLESS Trimeric Complex Represses
751 Flowering in Arabidopsis. *PLoS genetics* **12**(3): e1005959.
- 752 Guillen G, Diaz-Camino C, Loyola-Torres CA, Aparicio-Fabre R, Hernandez-Lopez A, Diaz-
753 Sanchez M, Sanchez F. 2013. Detailed analysis of putative genes encoding small
754 proteins in legume genomes. *Front Plant Sci* **4**.
- 755 Guttman M, Russell P, Ingolia NT, Weissman JS, Lander ES. 2013. Ribosome Profiling
756 Provides Evidence that Large Noncoding RNAs Do Not Encode Proteins. *Cell* **154**(1):
757 240-251.
- 758 Hanada K, Akiyama K, Sakurai T, Toyoda T, Shinozaki K, Shiu SH. 2010. sORF finder: a
759 program package to identify small open reading frames with high coding potential.
760 *Bioinformatics* **26**(3): 399-400.
- 761 Hanada K, Higuchi-Takeuchi M, Okamoto M, Yoshizumi T, Shimizu M, Nakaminami K, Nishi R,
762 Ohashi C, Iida K, Tanaka M et al. 2013. Small open reading frames associated with
763 morphogenesis are hidden in plant genomes. *P Natl Acad Sci USA* **110**(6): 2395-2400.
- 764 Hanada K, Zhang X, Borevitz JO, Li WH, Shiu SH. 2007. A large number of novel coding small
765 open reading frames in the intergenic regions of the Arabidopsis thaliana genome are
766 transcribed and/or under purifying selection. *Genome Res* **17**(5): 632-640.
- 767 Hazarika RR, De Coninck B, Yamamoto LR, Martin LR, Cammue BP, van Noort V. 2017. ARA-
768 PEPs: a repository of putative sORF-encoded peptides in Arabidopsis thaliana. *Bmc*
769 *Bioinformatics* **18**(1): 37.
- 770 Hellens RP, Brown CM, Chisnal MAW, Waterhouse PM, Macknight RC. 2016. The Emerging
771 World of Small ORFs. *Trends Plant Sci* **21**(4): 317-328.
- 772 Huang JZ, Chen M, Chen, Gao XC, Zhu S, Huang H, Hu M, Zhu H, Yan GR. 2017. A Peptide
773 Encoded by a Putative lncRNA HOXB-AS3 Suppresses Colon Cancer Growth. *Mol Cell*
774 **68**(1): 171-184 e176.
- 775 Iacono M, Mignone F, Pesole G. 2005. uAUG and uORFs in human and rodent 5'untranslated
776 mRNAs. *Gene* **349**: 97-105.
- 777 Ingolia NT, Lareau LF, Weissman JS. 2011. Ribosome Profiling of Mouse Embryonic Stem
778 Cells Reveals the Complexity and Dynamics of Mammalian Proteomes. *Cell* **147**(4):
779 789-802.
- 780 Johnstone TG, Bazzini AA, Giraldez AJ. 2016. Upstream ORFs are prevalent translational
781 repressors in vertebrates. *The EMBO journal* **35**(7): 706-723.

- 782 Karousis ED, Nasif S, Muhlemann O. 2016. Nonsense-mediated mRNA decay: novel
783 mechanistic insights and biological impact. *Wiley interdisciplinary reviews RNA* **7**(5):
784 661-682.
- 785 Kastenmayer JP, Ni L, Chu A, Kitchen LE, Au WC, Yang H, Carter CD, Wheeler D, Davis RW,
786 Boeke JD et al. 2006. Functional genomics of genes with small open reading frames
787 (sORFs) in *S-cerevisiae*. *Genome Res* **16**(3): 365-373.
- 788 Kim TS, Liu CL, Yassour M, Holik J, Friedman N, Buratowski S, Rando OJ. 2010. RNA
789 polymerase mapping during stress responses reveals widespread nonproductive
790 transcription in yeast. *Genome Biol* **11**(7): R75.
- 791 Kondo T, Plaza S, Zanet J, Benrabah E, Valenti P, Hashimoto Y, Kobayashi S, Payre F,
792 Kageyama Y. 2010. Small Peptides Switch the Transcriptional Activity of Shavenbaby
793 During *Drosophila* Embryogenesis. *Science* **329**(5989): 336-339.
- 794 Kozak M. 1986. Point mutations define a sequence flanking the AUG initiator codon that
795 modulates translation by eukaryotic ribosomes. *Cell* **44**(2): 283-292.
- 796 -. 1997. Recognition of AUG and alternative initiator codons is augmented by G in position +4
797 but is not generally affected by the nucleotides in positions +5 and +6. *The EMBO*
798 *journal* **16**(9): 2482-2492.
- 799 Kumar S, Stecher G, Suleski M, Hedges SB. 2017. TimeTree: A Resource for Timelines,
800 Timetrees, and Divergence Times. *Molecular biology and evolution* **34**(7): 1812-1819.
- 801 Ladoukakis E, Pereira V, Magny EG, Eyre-Walker A, Couso JP. 2011. Hundreds of putatively
802 functional small open reading frames in *Drosophila*. *Genome Biol* **12**(11).
- 803 Laing WA, Martinez-Sanchez M, Wright MA, Bulley SM, Brewster D, Dare AP, Rassam M,
804 Wang D, Storey R, Macknight RC et al. 2015. An Upstream Open Reading Frame Is
805 Essential for Feedback Regulation of Ascorbate Biosynthesis in *Arabidopsis*. *Plant Cell*
806 **27**(3): 772-786.
- 807 Lang D, Ullrich KK, Murat F, Fuchs J, Jenkins J, Haas FB, Piednoel M, Gundlach H, Van Bel M,
808 Meyberg R et al. 2018. The *Physcomitrella patens* chromosome-scale assembly
809 reveals moss genome structure and evolution. *Plant J* **93**(3): 515-533.
- 810 Laressergues D, Couzigou JM, Clemente HS, Martinez Y, Dunand C, Becard G, Combier JP.
811 2015. Primary transcripts of microRNAs encode regulatory peptides. *Nature*
812 **520**(7545): 90-93.
- 813 Lease KA, Walker JC. 2006. The *Arabidopsis* unannotated secreted peptide database, a
814 resource for plant peptidomics. *Plant Physiol* **142**(3): 831-838.
- 815 Ma J, Diedrich JK, Jungreis I, Donaldson C, Vaughan J, Kellis M, Yates JR, 3rd, Saghatelian A.
816 2016. Improved Identification and Analysis of Small Open Reading Frame Encoded
817 Polypeptides. *Analytical chemistry* **88**(7): 3967-3975.
- 818 Mackowiak SD, Zauber H, Bielow C, Thiel D, Kutz K, Calviello L, Mastrobuoni G, Rajewsky N,
819 Kempa S, Selbach M et al. 2015. Extensive identification and analysis of conserved
820 small ORFs in animals. *Genome Biol* **16**.
- 821 Magny EG, Pueyo JI, Pearl FM, Cespedes MA, Niven JE, Bishop SA, Couso JP. 2013. Conserved
822 regulation of cardiac calcium uptake by peptides encoded in small open reading
823 frames. *Science* **341**(6150): 1116-1120.
- 824 Matsumoto A, Pasut A, Matsumoto M, Yamashita R, Fung J, Monteleone E, Saghatelian A,
825 Nakayama KI, Clohessy JG, Pandolfi PP. 2017. mTORC1 and muscle regeneration are
826 regulated by the LINC00961-encoded SPAR polypeptide. *Nature* **541**(7636): 228-
827 232.
- 828 Mazin PV, Fisunov GY, Gorbachev AY, Kapitskaya KY, Altukhov IA, Semashko TA, Alexeev DG,
829 Govorun VM. 2014. Transcriptome analysis reveals novel regulatory mechanisms in a
830 genome-reduced bacterium. *Nucleic acids research* **42**(21): 13254-13268.
- 831 McLysaght A, Guerzoni D. 2015. New genes from non-coding sequence: the role of de novo
832 protein-coding genes in eukaryotic evolutionary innovation. *Philosophical*

- 833 *transactions of the Royal Society of London Series B, Biological sciences* **370**(1678):
834 20140332.
- 835 Montoya-Burgos JI. 2011. Patterns of positive selection and neutral evolution in the protein-
836 coding genes of Tetraodon and Takifugu. *Plos One* **6**(9): e24800.
- 837 Moyers BA, Zhang J. 2016. Evaluating Phylostratigraphic Evidence for Widespread De Novo
838 Gene Birth in Genome Evolution. *Molecular biology and evolution* **33**(5): 1245-1256.
- 839 Narita NN, Moore S, Horiguchi G, Kubo M, Demura T, Fukuda H, Goodrich J, Tsukaya H. 2004.
840 Overexpression of a novel small peptide ROTUNDIFOLIA4 decreases cell proliferation
841 and alters leaf shape in Arabidopsis thaliana. *Plant J* **38**(4): 699-713.
- 842 Neafsey DE, Galagan JE. 2007. Dual modes of natural selection on upstream open reading
843 frames. *Molecular biology and evolution* **24**(8): 1744-1751.
- 844 Nelson BR, Makarewich CA, Anderson DM, Winders BR, Troupes CD, Wu F, Reese AL,
845 McAnally JR, Chen X, Kavalali ET et al. 2016. A peptide encoded by a transcript
846 annotated as long noncoding RNA enhances SERCA activity in muscle. *Science*
847 **351**(6270): 271-275.
- 848 Nishiyama T, Hiwatashi Y, Sakakibara I, Kato M, Hasebe M. 2000. Tagged mutagenesis and
849 gene-trap in the moss, Physcomitrella patens by shuttle mutagenesis. *DNA research :
850 an international journal for rapid publication of reports on genes and genomes* **7**(1): 9-
851 17.
- 852 Paytavi Gallart A, Hermoso Pulido A, Anzar Martinez de Lagran I, Sanseverino W, Aiese
853 Cigliano R. 2016. GREENC: a Wiki-based database of plant lncRNAs. *Nucleic acids
854 research* **44**(D1): D1161-1166.
- 855 Pi H, Lee LW, Lo SJ. 2009. New insights into polycistronic transcripts in eukaryotes. *Chang
856 Gung medical journal* **32**(5): 494-498.
- 857 Popp MW, Maquat LE. 2013. Organizing principles of mammalian nonsense-mediated mRNA
858 decay. *Annual review of genetics* **47**: 139-165.
- 859 Prabakaran S, Hemberg M, Chauhan R, Winter D, Tweedie-Cullen RY, Dittrich C, Hong E,
860 Gunawardena J, Steen H, Kreiman G et al. 2014. Quantitative profiling of peptides
861 from RNAs classified as noncoding. *Nature communications* **5**: 5429.
- 862 Rasheed S, Bashir K, Nakaminami K, Hanada K, Matsui A, Seki M. 2016. Drought stress
863 differentially regulates the expression of small open reading frames (sORFs) in
864 Arabidopsis roots and shoots. *Plant signaling & behavior* **11**(8): e1215792.
- 865 Rensing SA, Ick J, Fawcett JA, Lang D, Zimmer A, Van de Peer Y, Reski R. 2007. An ancient
866 genome duplication contributed to the abundance of metabolic genes in the moss
867 Physcomitrella patens. *BMC evolutionary biology* **7**: 130.
- 868 Rensing SA, Lang D, Zimmer AD, Terry A, Salamov A, Shapiro H, Nishiyama T, Perroud PF,
869 Lindquist EA, Kamisugi Y et al. 2008. The Physcomitrella genome reveals
870 evolutionary insights into the conquest of land by plants. *Science* **319**(5859): 64-69.
- 871 Rohrig H, Schmidt J, Miklashevichs E, Schell J, John M. 2002. Soybean ENOD40 encodes two
872 peptides that bind to sucrose synthase. *Proc Natl Acad Sci U S A* **99**(4): 1915-1920.
- 873 Samandi S, Roy AV, Delcourt V, Lucier JF, Gagnon J, Beaudoin MC, Vanderperre B, Breton MA,
874 Motard J, Jacques JF et al. 2017. Deep transcriptome annotation enables the discovery
875 and functional characterization of cryptic small proteins. *eLife* **6**.
- 876 Schaefer DG, Zryd JP. 1997. Efficient gene targeting in the moss Physcomitrella patens. *Plant
877 J* **11**(6): 1195-1206.
- 878 Seo PJ, Hong SY, Kim SG, Park CM. 2011. Competitive inhibition of transcription factors by
879 small interfering peptides. *Trends Plant Sci* **16**(10): 541-549.
- 880 Seo PJ, Park MJ, Park CM. 2013. Alternative splicing of transcription factors in plant
881 responses to low temperature stress: mechanisms and functions. *Planta* **237**(6):
882 1415-1424.

- 883 Slavoff SA, Mitchell AJ, Schwaid AG, Cabili MN, Ma J, Levin JZ, Karger AD, Budnik BA, Rinn JL,
884 Saghatelian A. 2013. Peptidomic discovery of short open reading frame-encoded
885 peptides in human cells. *Nat Chem Biol* **9**(1): 59-+.
- 886 Staudt AC, Wenkel S. 2011. Regulation of protein function by 'microProteins'. *EMBO reports*
887 **12**(1): 35-42.
- 888 Supek F, Bosnjak M, Skunca N, Smuc T. 2011. REVIGO summarizes and visualizes long lists of
889 gene ontology terms. *Plos One* **6**(7): e21800.
- 890 Suyama M, Torrents D, Bork P. 2006. PAL2NAL: robust conversion of protein sequence
891 alignments into the corresponding codon alignments. *Nucleic acids research* **34**(Web
892 Server issue): W609-612.
- 893 Szczesniak MW, Rosikiewicz W, Makalowska I. 2016. CANTATAdb: A Collection of Plant Long
894 Non-Coding RNAs. *Plant Cell Physiol* **57**(1): e8.
- 895 Tautz D. 2009. Polycistronic peptide coding genes in eukaryotes--how widespread are they?
896 *Briefings in functional genomics & proteomics* **8**(1): 68-74.
- 897 Tavormina P, De Coninck B, Nikonorova N, De Smet I, Cammue BP. 2015. The Plant
898 Peptidome: An Expanding Repertoire of Structural Features and Biological Functions.
899 *Plant Cell* **27**(8): 2095-2118.
- 900 Tyanova S, Temu T, Cox J. 2016. The MaxQuant computational platform for mass
901 spectrometry-based shotgun proteomics. *Nat Protoc* **11**(12): 2301-2319.
- 902 van der Lee R, Buljan M, Lang B, Weatheritt RJ, Daughdrill GW, Dunker AK, Fuxreiter M,
903 Gough J, Gsponer J, Jones DT et al. 2014. Classification of intrinsically disordered
904 regions and proteins. *Chemical reviews* **114**(13): 6589-6631.
- 905 Vanderperre B, Lucier JF, Bissonnette C, Motard J, Tremblay G, Vanderperre S, Wisztorski M,
906 Salzet M, Boisvert FM, Roucou X. 2013. Direct Detection of Alternative Open Reading
907 Frames Translation Products in Human Significantly Expands the Proteome. *Plos One*
908 **8**(8).
- 909 Verheggen K, Volders PJ, Mestdagh P, Menschaert G, Van Damme P, Gevaert K, Martens L,
910 Vandesompele J. 2017. Noncoding after All: Biases in Proteomics Data Do Not Explain
911 Observed Absence of lncRNA Translation Products. *J Proteome Res* **16**(7): 2508-2515.
- 912 Vizcaino JA, Csordas A, Del-Toro N, Dianes JA, Griss J, Lavidas I, Mayer G, Perez-Riverol Y,
913 Reisinger F, Ternent T et al. 2016. 2016 update of the PRIDE database and its related
914 tools. *Nucleic acids research* **44**(22): 11033.
- 915 Xu H, Wang P, Fu Y, Zheng Y, Tang Q, Si L, You J, Zhang Z, Zhu Y, Zhou L et al. 2010. Length of
916 the ORF, position of the first AUG and the Kozak motif are important factors in
917 potential dual-coding transcripts. *Cell research* **20**(4): 445-457.
- 918 Yang Z. 2007. PAML 4: phylogenetic analysis by maximum likelihood. *Molecular biology and*
919 *evolution* **24**(8): 1586-1591.
- 920 Ye J, Coulouris G, Zaretskaya I, Cutcutache I, Rozen S, Madden TL. 2012. Primer-BLAST: a tool
921 to design target-specific primers for polymerase chain reaction. *Bmc Bioinformatics*
922 **13**: 134.
- 923 Zhang L, Li WH. 2004. Mammalian housekeeping genes evolve more slowly than tissue-
924 specific genes. *Molecular biology and evolution* **21**(2): 236-239.
- 925

926

927 **FIGURE LEGENDS**

928 **Fig. 1. Several distinct types of sORFs are present in the moss genome. A** – Pipeline used in this
929 study to identify coding sORFs; **B** – Proposed classification of sORFs according to the types of

930 encoding transcripts: upstream ORFs (uORFs) and downstream ORFs (dORFs) in the untranslated
931 regions (UTRs) of canonical mRNAs; CDS-sORFs, which overlap with protein-coding sequences in
932 alternative (+2 or +3) reading frames or are truncated versions of proteins generated by alternative
933 splicing; interlaced-sORFs, which overlap both the protein-coding sequence and UTR on the same
934 transcript; lncRNA-sORFs and intergenic sORFs, which are located on short non-protein coding
935 transcripts.; **C** – Boxplot of the length distribution of sORFs in different groups; **D** – The results of GO
936 enrichment analysis for genes possessing uORFs and CDS-sORFs. BP, CC and MF represent “Biological
937 process”, “Cellular component” and “Molecular function”, respectively.

938 **Fig. 2. Analysis of the trends in sORFs evolution.** **A** – The percentage of each type of sORF among
939 sORFs having homologs in ten plant species. **B** – Statistical analysis (by Fisher’s exact test) of
940 differences between the number of conservative sORFs in each of ten species and the initial dataset;
941 **C** – Pairwise K_A/K_S ratio distribution for each type of sORF conserved among ten plant species.

942 **Fig. 3. Moss contains hundreds of translatable sORFs.** **A** – Venn diagram showing the distribution
943 of the identified sORFs among three types of moss cells; **B** - Distribution of translatable sORFs based
944 on the suggested classification; **C** - Length distribution of various groups of translatable sORFs; **D** -
945 Heatmap showing expression levels ($\log_{10}(\text{RPKM})$) for the lncRNAs (left) carrying sORFs (lncRNA-
946 sORFs) and binary heatmap showing evidence of translation (determined as whether a peptide was
947 identified (brown) or not (grey) in MS data) for the corresponding lncRNA-sORFs (right) in three
948 moss tissues, gametophores (G), protonemata (N) and protoplasts (P) ; **E** – Binary heatmap showing
949 evidence of translation for sORFs and proteins in multicoding genes in three moss tissues. G, N and P
950 correspond to gametophores, protonemata and protoplasts, respectively. **F** - Examples of contrasting
951 translational patterns of the main ORF and CDS-sORF. Only proteins confirmed by more than three
952 unique tryptic peptides in the MS data are shown.

953 **Fig. 4. Alternative splicing regulates the expression of sORFs.** **A** – Enrichment analysis of
954 different sORF groups in a set of AS-sORFs and AS-REFs. P-value was calculated by Fisher’s exact test.
955 ***P < 1e-10; **P < 0.001; *P < 0.05; **B** – Venn diagram showing the number of AS-sORFs influenced
956 by different AS events. **C** – Example of a translatable CDS-sORF, which was generated by an AS event
957 and partially overlaps with the main ORF of Pp3c11_17810. Intron retention caused the formation of

958 the isoform with the sORF, while splicing of this intron led to the excision of the sORF stop codon and
959 its disruption. MS detection of the peptide located at the exon-AS-intron junction allowed the
960 translation of the sORF to be unambiguously distinguished from the translation of the main ORF.
961 Upper panel shows the amino acid sequence of the sORF-encoded peptide, MS detected peptide and
962 (partial) protein translated from the main ORF. Black and gray dotted lines mark the borders of the
963 sORF and the canonical intron start site, respectively. The intron-exon structure of three transcript
964 isoforms of the gene was retrieved from Phytozome (v12).

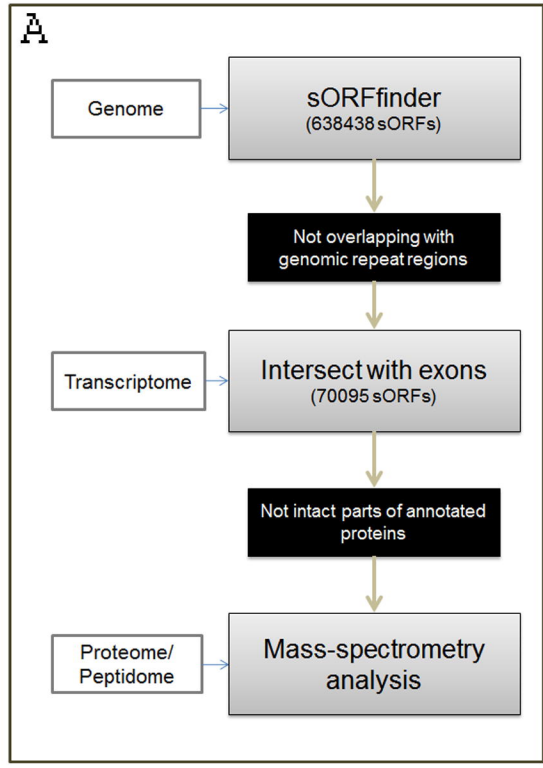
965 **Fig. 5. Morphology of wild type and sORF-encoded peptide mutant lines. The phenotypes of**
966 **PSEP1 knockout (KO) and overexpression (OE) lines grown on BCD medium with 0.5%**
967 **glucose:** A, D – overexpression of PSEP1; C, F – knockout of PSEP1; G – the diameter of moss plants
968 with overexpression and knockout of sORF-encoded peptide PSEP1. **The phenotypes of PSEP3**
969 **knockout (KO) lines grown on BCD medium:** H, J – wild type; I, K – knockout lines; L - the diameter
970 of moss plants with knockout of PSEP3. **The phenotypes of PSEP25 knockout (KO) lines grown**
971 **on BCDAT medium:** M, O, Q – wild type; N, P, R – knockout lines; S - the diameter of moss plants
972 with knockout of PSEP25. T – the number of leafy gametophores in wild type and three PSEP25
973 knockout lines. Arrows show young leafy gametophores. Scale bar: 500 μ m. P-value was calculated
974 by Student's t-test. **P < 0.01; *P < 0.05.

975 **Fig. 6. Proposed functions of sORF-encoded peptides.** A – uORFs can function in the regulation of
976 translation of the downstream main ORF. The functions of peptides encoded by uORFs are unknown,
977 and most are likely to represent “noise” from protein translation; B – CDS-sORF-encoded peptides
978 can help regulate protein-protein interactions, and some interfere with the translation of the main
979 ORF; C – long non-coding RNAs or intergenic-sORFs can produce biologically active peptides that
980 perform signaling, defense or regulatory functions. In addition, the translation of sORFs can activate
981 the nonsense-mediated decay (NMD) mechanism, which leads to the degradation of the
982 corresponding transcripts.

983

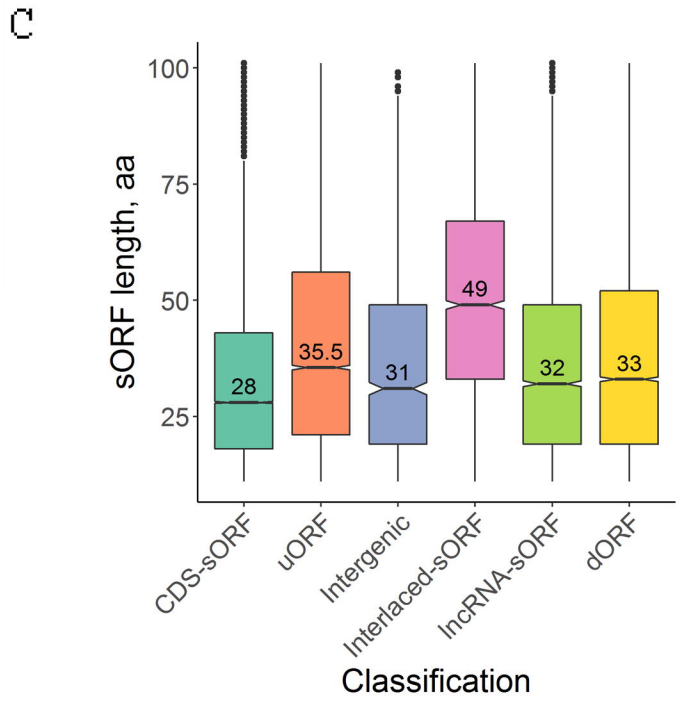
984

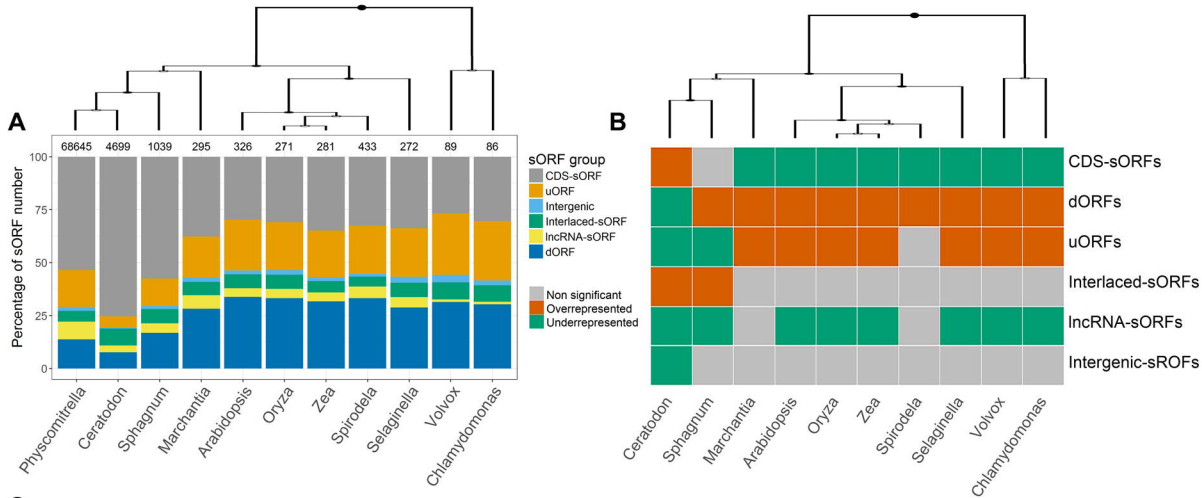
985

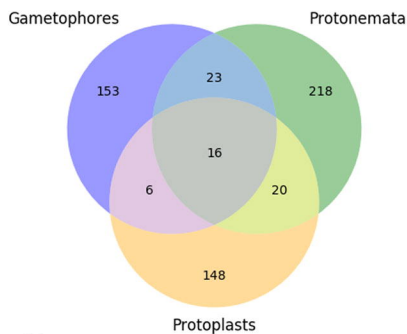
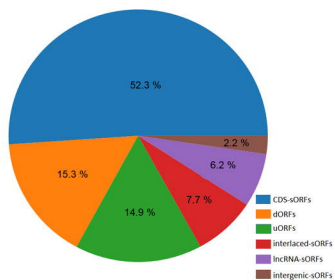
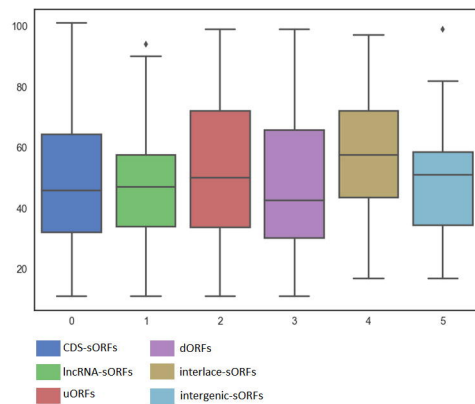
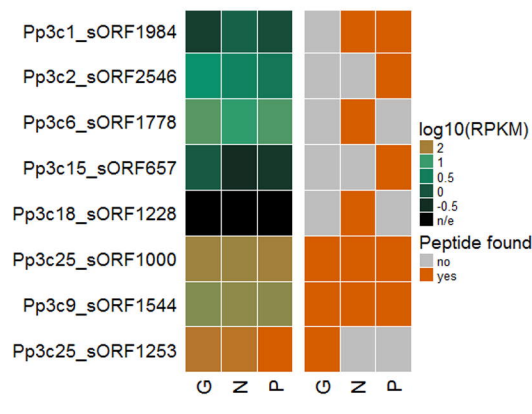
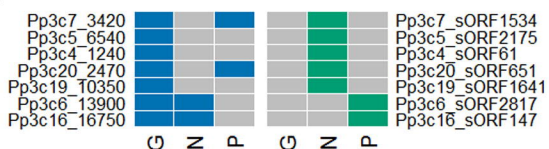
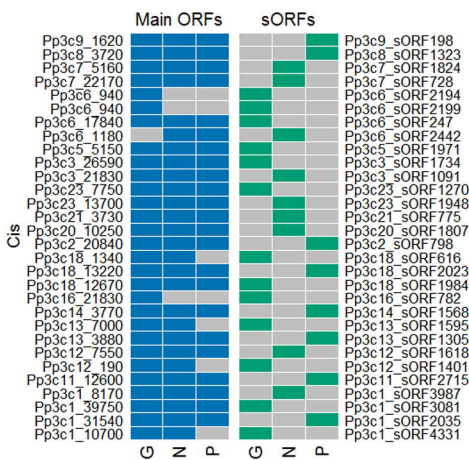


B

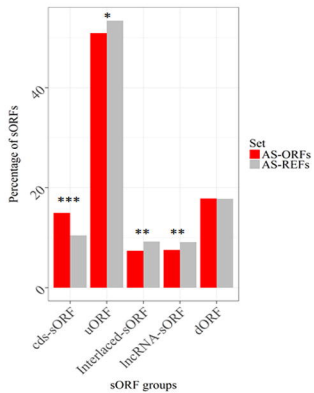
sORF class	RNA type	Evidence of transcription (RNA-seq data)	Evidence of translation (MS data)
Upstream sORFs (uORFs)	5'-AAAA-3'	11998	92
Downstream sORFs (dORFs)	5'-AAAA-3'	9444	93
Coding sequence-sORFs (CDS-sORFs)	5'-AAAA-3'	36732	312
Interlaced-sORFs	5'-AAAA-3'	3485	45
Intergenic/ lncRNA-sORFs	5'-AAAA-3'	1241/5745	13/36



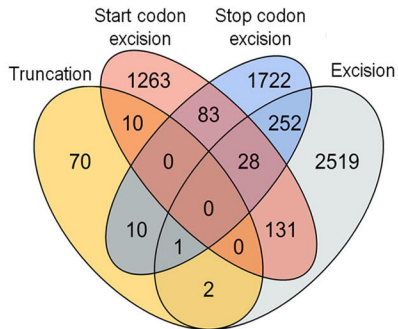


A**B****C****D****F****E**

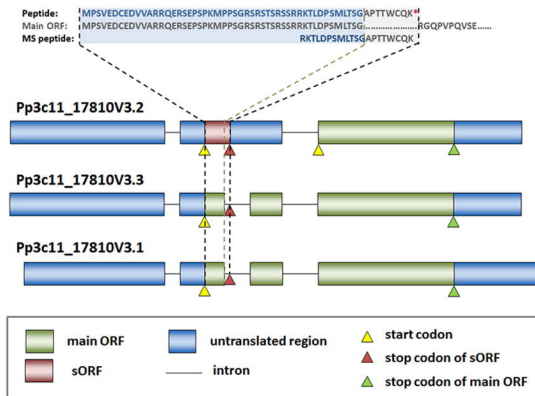
A

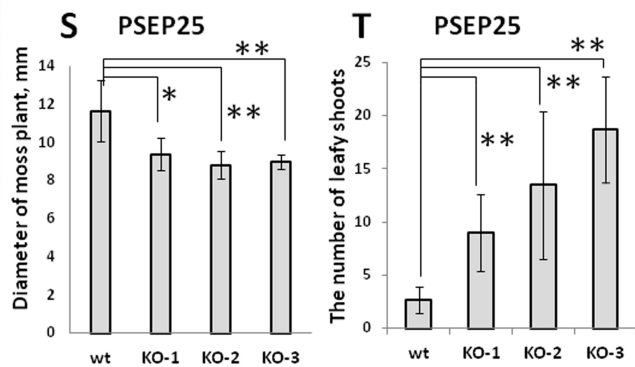
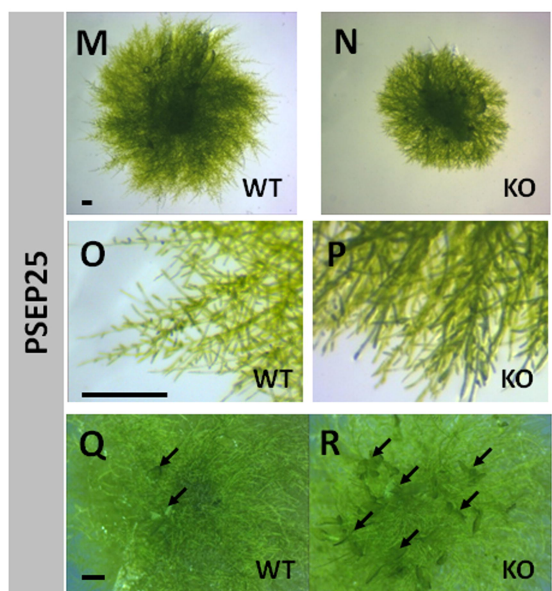
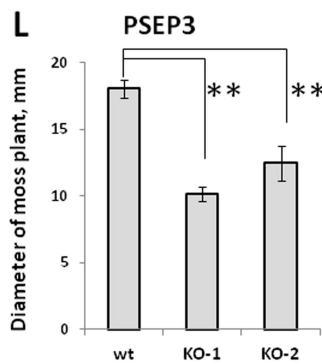
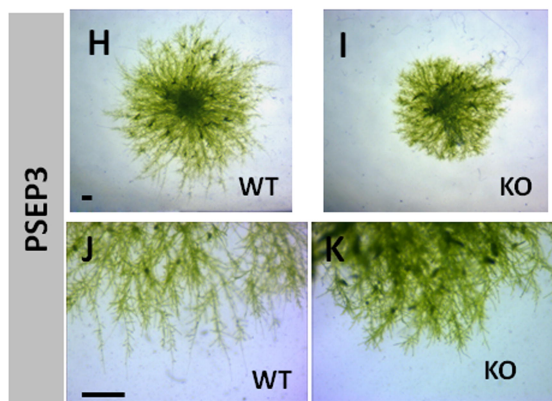
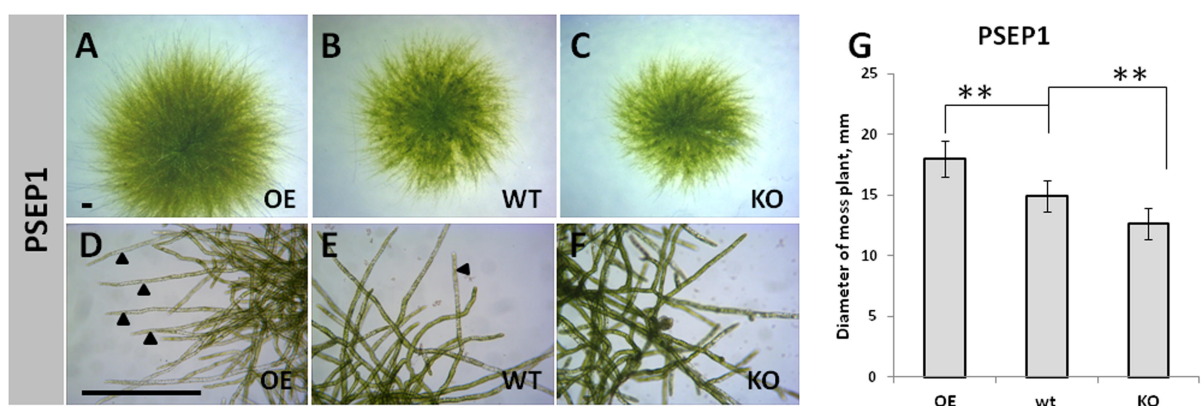


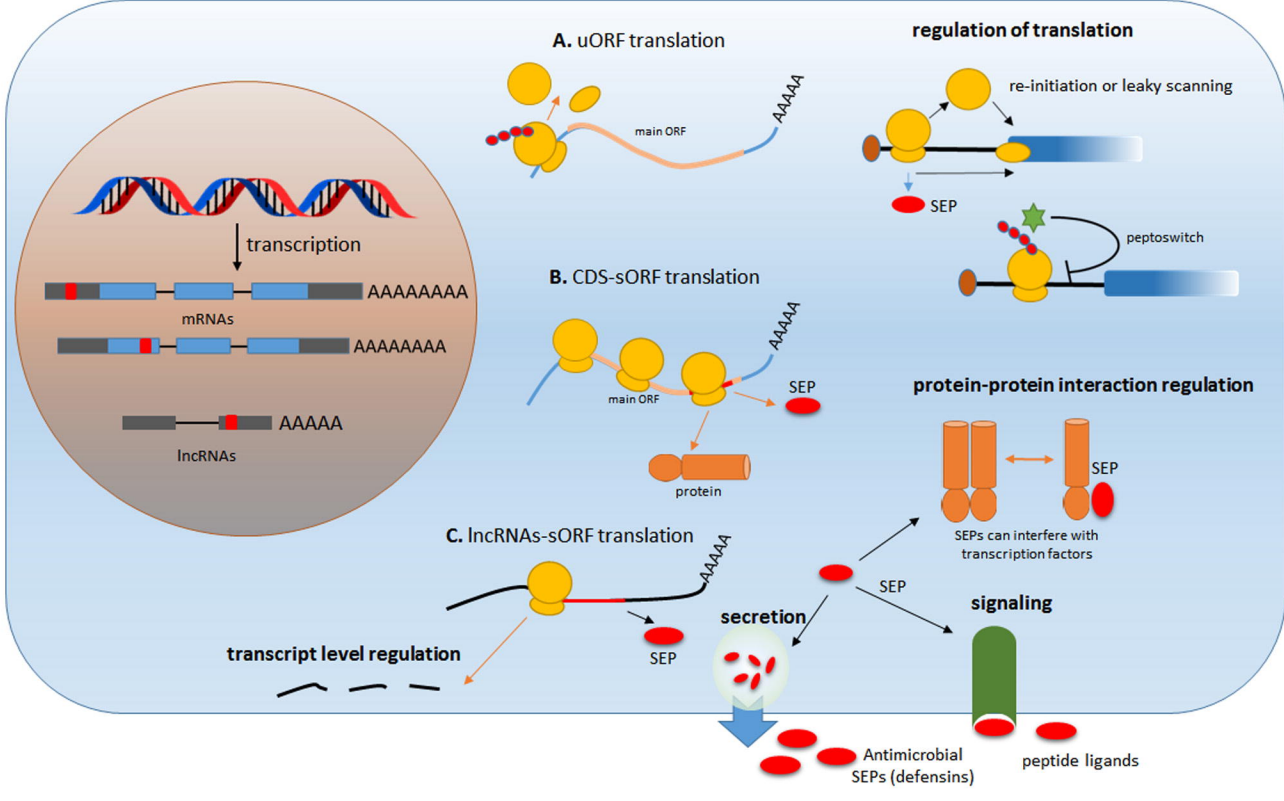
B



C







Antimicrobial SEPs (defensins) peptide ligands